Structures 10 (2017) 89–95

Contents lists available at ScienceDirect

Structures

journal homepage: www.elsevier.com/locate/structures

Behavior of Concrete Filled Elliptical Steel Tubular Deep Beam under Bending-Shear

Kojiro Uenaka [a,*], Hisao Tsunokake [b]

[a] Department of Civil Engineering, Kobe City College of Technology, Gakuenhigashimachi 8-3, Nishi, Kobe 6512194, Japan.
[b] Department of Urban Engineering, Osaka City University, Sugimoto 3-3-138, Sumiyoshi, Osaka, 5588585, Japan

ARTICLE INFO

Article history:
Received 23 October 2016
Received in revised form 1 February 2017
Accepted 10 February 2017
Available online 16 February 2017

Keywords:
CFEST
CFT
Bending-shear capacity
Asymmetric four-point loading test
Large diameter-to-thickness ratio
Principal stress behavior

ABSTRACT

A concrete filled elliptical steel tubular, abbreviated as CFEST, member consists of an elliptical hollow steel tube and in-filled concrete. The CFEST member is a family of concrete filled steel tubular (CFT) member having large deformability and toughness due to the confinement effect between the steel tube and the in-filled concrete. When the CFEST member is applied to bridge piers in the river, reduction of the bottom scouring due to the water flow can be expected.

The present study aims to investigate, experimentally, the bending shear characteristics of CFEST deep beams through asymmetric four-point loading test method. The selected testing parameters are diameter-to-thickness ratio and two loading directions, namely the major and the minor axes. The results showed that shear capacity of CFEST members is strongly affected by the diameter-to-thickness ratio. The observed failure modes were cracking of the tube and/or shear failure of the in-filled concrete. A method to predict simple shear capacity of the CFEST deep beam is mainly discussed. Additionally, elasto-plastic principal stress behavior of the steel tube is also mentioned.

© 2017 Institution of Structural Engineers. Published by Elsevier Ltd. All rights reserved.

1. Introduction

Concrete filled elliptical steel tubular, so-called CFEST or concrete-filled EHS, members consist of an elliptical steel tube filled in with concrete, as shown in Fig. 1. The CFEST is a family of the concrete filled steel tubular (CFT) members [1–2] having good deformability and large toughness owing to the confinement effect between the steel tube and the in-filled concrete. Moreover, when CFEST member is applied to bridge piers in a river, allowing a smooth water flow around them, reduction of scouring on the riverbed can be expected.

So far, there have been various investigations on mechanical behavior of concrete filled and unfilled elliptical hollow steel sections (EHS) and oval hollow sections (OHS) as follows. First, hot-rolled elliptical hollow section stub column test under compression was carried out by Chan and Gardner [3]. Symmetric three- and four-point loading test on hollow elliptical steel tubular beams under bending-shear was performed by Gardner et al. [4] and Chan and Gardner [5], followed by Ruiz-Teran & Gardner [6] and Gardner & Chan [7] who conducted buckling analysis on elliptical hollow steel tubes. As for researches on the CFEST, stub column under centric compression [8–10] and combination of axial force and bending moment [11–12] tests were carried out. Moreover, Ren QX et al. [13] discussed symmetric four-point loading test on CFEST beam. However, these previous researches focused on larger diameter-to-thickness ratio ($2a/t$) of the EHS or OHS, ranging from 28 to 40. To apply CFEST members to high-rise bridge pier, it is important to investigate CFEST members having large diameter-to-thickness ratio that are larger than 100.

Under the above-described background, we have conducted two systematic studies on the CFEST members with large diameter-to-thickness ratio that are larger than 100 to be applied to the bridge piers in riverbeds, namely, the centric loading [14] and the pure bending tests [15]. From the results, it can be stated that the two experimental strengths decreased as diameter-to-thickness ratio of elliptical steel tube increased. In addition, the methods to predict centric loading and pure bending capacities of CFEST were mainly discussed.

The present study aims to investigate, experimentally, the shear characteristics of CFEST deep beams with large diameter-to-thickness ratio ($2a/t$) ranging from 69 to 160 through asymmetric four-point loading test. The selected testing parameters are diameter-to-thickness ratio ($2a/t$) and loading directions (major and minor axes). A Method to predict simple shear strength of the CFEST deep beam is mainly discussed. Moreover, comparison between ordinary circular CFT and CFEST specimens is also made. In addition, principal stress behavior of the steel tubes induced by in-filled concrete is also mentioned. Part of this study has been previously reported in Japan [16].

* Corresponding author.
E-mail address: uenaka@kobe-kosen.ac.jp (K. Uenaka).

http://dx.doi.org/10.1016/j.istruc.2017.02.002
2352-0124/© 2017 Institution of Structural Engineers. Published by Elsevier Ltd. All rights reserved.

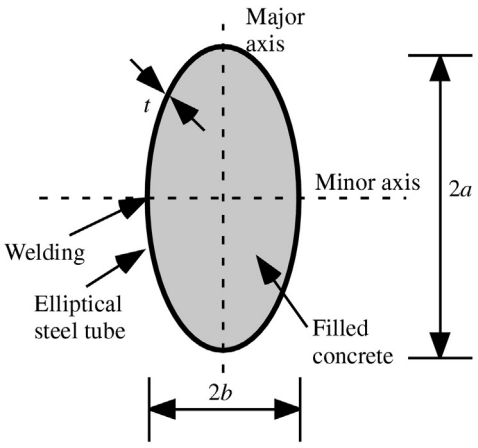

Fig. 1. Cross sections of CFEST.

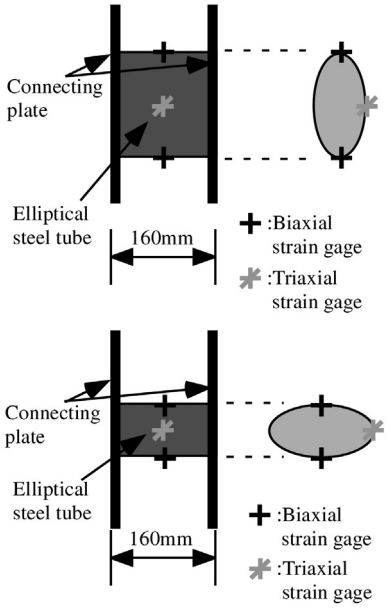

Fig. 2. Details of the specimens.

2. Experimental testing

2.1. Test specimens

Table 1 summarizes the details of the test specimens, including that of circular CFT beam. The length/larger diameter ratio and the aspect ratio of elliptical steel tubes are 160 mm and 2.0, respectively, as shown in Figs. 1 and 2. The thicknesses of the steel tubes are 1.0, 1.6 and 2.3 mm. Therefore, larger diameter-to-thickness ratios ($2a/t$) of the elliptical steel tubes varies from 69 to 160. Whereas, six specimens of concrete filled circular steel tubular (CFT) deep beams are prepared in order to be compared with the CFEST deep beam. The elliptical and circular steel tubes fabricated out of 1.0, 1.6 and 2.3 mm steel plates had longitudinal welded seam. The elliptical and circular steel tubes had strengthening plates at both ends which were connected to the side beams by 10 high-strength bolts.

The loading method and the bending moment and shear force diagrams are shown in Fig. 3. Constant shear force is applied to the CFEST deep beam through the asymmetric four-point loading testing method as shown in Fig. 3. Therefore, detailed bending and shear actions are applied to the specimens as shown in Fig. 4. Additionally, this loading action can be assumed as the CFEST bridge pier. Fig. 5 shows the 500kN universal tester of the test apparatus located in Kobe City College of Technology. The experimental program was completed when failure occurred.

2.2. Measurements

Two biaxial and one triaxial strain gages were attached on the surface of the steel tubes to obtain the stress conditions of the elliptical steel tubes as shown in Fig. 2. Two displacement transducers were placed under the CFEST specimens to obtain shear deformation as shown in Fig. 3.

3. Results and discussion

3.1. Failure modes

Fig. 6(a) and (b) show the observed failure modes of the CFEST deep beams. In both specimen types, namely, CFEST and circular CFT, cracking of the steel tubes in the tensile region was found. In addition, shear failure of in-filled concrete between the loading point and the supports may be assumed as shown in Fig. 6(a). This finding coincided with CFT deep beam bending-shear test, which has been previously reported [17].

Table 1
List of the specimens.

No.	Tag	Steel tube							Concrete strength
		Thick.	Diameter		Ratio		Yielding point	Fracture point	
		t (mm)	$2a$ (mm)	$2b$ (mm)	$2a/t$	$2\,b/t$	f_y (N/mm^2)	f_u (N/mm^2)	f_c' (N/mm^2)
1	s10-major	1.0	160.0	80.0	160.0	80.0	196.0	345.4	34.9
2	s10-minor	1.0	160.0	80.0	160.0	80.0	196.0	345.4	
3	s16-major	1.6	160.0	80.0	100.0	50.0	313.3	358.0	
4	s16-minor	1.6	160.0	80.0	100.0	50.0	313.3	358.0	
5	s23-major	2.3	160.0	80.0	69.6	34.8	298.7	373.4	
6	s23-minor	2.3	160.0	80.0	69.6	34.8	298.7	373.4	
7	s10–80	1.0	80.0	80.0	80.0	80.0	196.0	345.4	34.9
8	s10–160	1.0	160.0	160.0	160.0	160.0	196.0	345.4	
9	s16–80	1.6	80.0	80.0	50.0	50.0	313.3	358.0	
10	s16–160	1.6	160.0	160.0	100.0	100.0	313.3	358.0	
11	s23–80	2.3	80.0	80.0	34.8	34.8	298.7	373.4	
12	s23–160	2.3	160.0	160.0	69.6	69.6	298.7	373.4	

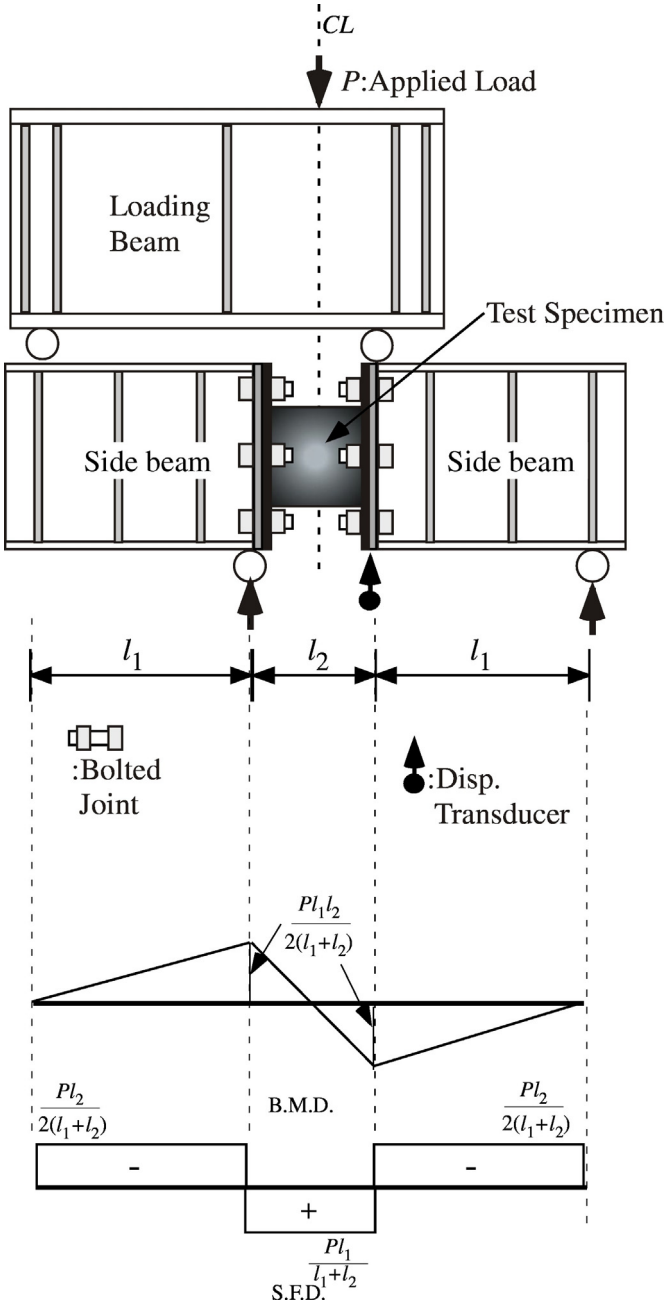

Fig. 3. Asymmetric four-point loading test.

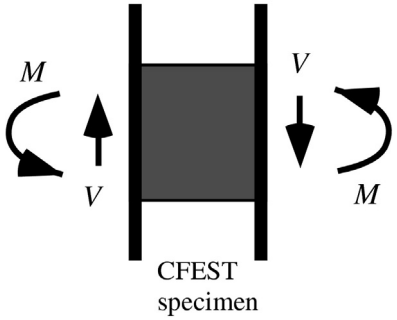

Fig. 4. Detailed loading condition.

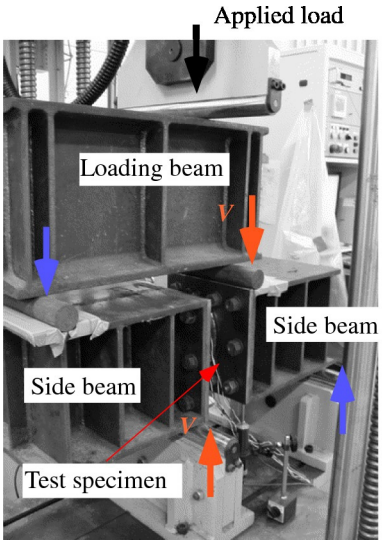

Fig. 5. Test apparatus.

On the other hand, with respect to the minor test and CFT with $D =$ 80 mm specimens, no shear failure of in-filled concrete between the two supports was assumed, as shown in Fig. 6(b). This is because the shear span ratio of the minor test and CFT with $D = 80$ mm is two times larger than that of the major test and CFT with $D = 160$ mm specimens.

3.2. Shear strength

3.2.1. Experimental shear capacity

Fig. 7 shows the relationship between shear strength (V_{exp}) and larger diameter-to-thickness ratio ($2a/t$) of the steel tube. In all test results, it can be noted that the shear strength decreased as $2a/t$ increased. This is attributed to reduction of cross sectional area of the elliptical steel tube. This phenomenon coincided with pure bending test results of CFEST beam through symmetric four-point loading [15].

3.2.2. Shear capacity prediction

First, in order to simplify the estimation of shear strength of deep CFEST beam, cross sectional area of the CFEST is transformed into a rectangular section having equivalent cross sectional area (A_s) and thickness (t) of the elliptical steel tubes, as shown in Fig. 8.

Shear strength of the deep RC beam proposed by Niwa [17] is expressed as below,

$$V_u = \frac{0.24 f_c'^{\frac{2}{3}}\left(1+\sqrt{100 p_w}\right)\left(1+3.33\frac{r_p}{d}\right)}{1+\left(\frac{a_s}{d}\right)^2} b_w d \tag{1}$$

where f_c': concrete strength, a_s: shear span length ($=80$ mm) and r_p: width of loading plate ($=12$ mm). From Fig. 8, the width (b_w) and the effective depth (d) can be expressed as below.

$$b_w = \frac{A_s}{2t} - 2a + 2t \text{ and } d = 2a - \frac{t}{2} \text{ (for major test)} \tag{2a}$$

$$b_w = \frac{A_s}{2t} - 2b + 2t \text{ and } d = 2b - \frac{t}{2} \text{ (for minor test)} \tag{2b}$$

According to the Truss Theory of RC deep beam, shear strength of the steel tubes can be expressed as below,

$$V_s = 2dtf_y \tag{3}$$

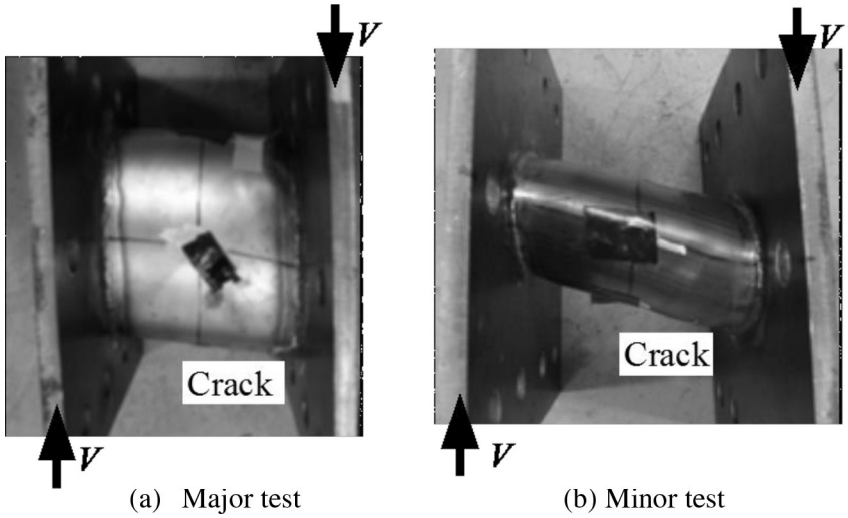

Fig. 6. Failure modes.

The simply predicted shear strength ($V_{est\text{-}R}$) is the sum of Eqs. (1) and (3), that is

$$V_{est-R} = V_u + V_s \tag{4}$$

The values of the predicted strengths ($V_{est\text{-}R}$) calculated by Eq. (4) are summarized in Table 2.

In Fig. 9, experimental shear strengths (V_{exp}) of CFEST and CFT are plotted against the predicted shear strength ($V_{est\text{-}R}$) calculated according to Eq. (4). In the figure, experimental shear strength previously reported [18] is included. The predicted shear strength ($V_{est\text{-}R}$) corresponded well with the experimental strength V_{exp} as shown in Fig. 9, where the strength ratio $V_{exp}/V_{est\text{-}R}$ and their good correlation factor are 0.99 and 0.94, respectively, according to the least-square method. It can be noted that shear strength of CFEST deep beam can be predicted by rectangular CFT members having depth equivalent to that of a rectangular section and cross sectional area of CFEST with in-filled concrete.

3.3. Bending strength

According to [15], CFEST beam subjected to bending moment (M_{est}) and axial load (N_{est}) can be calculated as below,

$$M_{est} = \frac{2}{3}kf'_c(a-t)(b-t)^2\cos^3\alpha + \frac{4}{3}f_y\left\{ab^2-(a-t)(b-t)^2\right\}\cos^3\alpha \tag{5}$$

$$N_{est} = \frac{kf'_c}{2}(a-t)(b-t)(\pi-2\alpha-\sin 2\alpha) - f_y t(a+b-t)(\sin 2\alpha + 2\alpha) \tag{6}$$

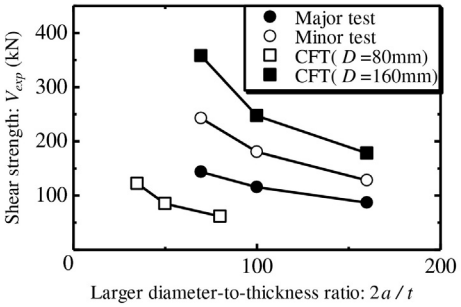

Fig. 7. Shear strength.

where α: angle from neutral axis to the bottom of the compressive area, k: concrete reduction factor (=0.85). The confinement effect of in-filled concrete is neglected.

Fig. 10 gives the experimental bending strength (M_{exp}) against the estimated bending strength (M_{est}), in which the angle α is obtained from $N_{est} = 0$. Fig. 9 also includes previous CFT test results [18]. From the Fig. 10, the estimated bending strength (M_{est}) is, either in good agreement with, or larger than, the estimations, being the correlation factor and the ratio M_{exp}/M_{est} equal to 0.92 and 1.17, respectively, according to the least-square method.

3.4. Shear deformability

Fig. 11(a) and (b) show shear load (V) of major and minor tests against the corresponding shear deflection (δ) divided by specimen's height (H = 160 mm). From the figures, it can be found that shear deformability of CFEST deep beams decreased as diameter-to-thickness

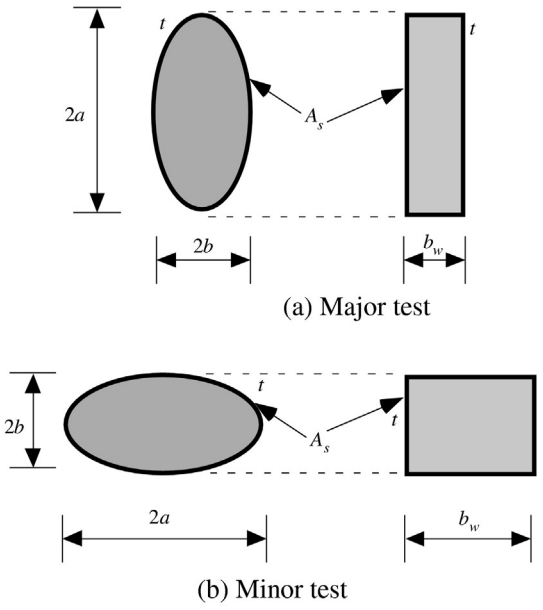

Fig. 8. Transformations of cross sections.

Table 2
Experiments and estimations.

No.	Tag.	d (mm)	V_{exp} (kN)	$V_{est\text{-}R}$ (kN)
1	s10-major	159.5	128.0	83.7
2	s10-minor	79.5	86.8	66.3
3	s16-major	159.2	180.4	183.4
4	s16-minor	79.2	115.4	119.4
5	s23-major	158.9	242.5	244.7
6	s23-minor	78.9	143.6	152.8
7	s10-80	79.5	61.4	46.0
8	s10-160	159.5	177.9	129.7
9	s16-80	79.2	84.9	96.4
10	s16-160	159.2	247.0	234.7
11	s23-80	78.9	122.1	127.3
12	s23-160	158.9	357.6	300.9

ratio ($2a/t$) increased. This is mainly due to the reduction of cross sectional area of the steel tubes. Whereas, Fig. 11(c) gives the relationship between shear load (V) and shear deformability of the specimens having $t = 1.6$ mm. From the figure, it can be observed that shear load (V) of the specimens kept maximum displacement values of over 5%, approximately.

3.5. Principal stress behavior

3.5.1. Calculation of biaxial stress [19]

A triaxial strain gage is attached on the external side of the steel tubes, as shown in Fig. 2. According to von Mises criteria, yielding stress under plane stress conditions can be calculated as below,

$$f_s = \sigma_1^2 - \sigma_1 \cdot \sigma_2 + \sigma_2^2 - f_y^2 \tag{7}$$

where, σ_1 and σ_2 are the two principal stresses of the steel tube. When the two stresses are within the elastic range, that is, $f_s < 0$, their stresses can be calculated as below,

$$\begin{Bmatrix} d\sigma_1 \\ d\sigma_2 \end{Bmatrix} = \frac{E}{1-\nu^2}\begin{bmatrix} 1 & \nu \\ \nu & 1 \end{bmatrix}\begin{Bmatrix} d\varepsilon_1 \\ d\varepsilon_2 \end{Bmatrix} \tag{8}$$

where ε_1 and ε_2 are the two principal strains, E and ν are the Young's modulus and the Poisson's ratio of the steel tubes, respectively.

When the two stresses enter the plastic range, that is, $f_s = 0$, elasto-plastic stress can be calculated as below,

$$\begin{Bmatrix} d\sigma_1 \\ d\sigma_2 \end{Bmatrix} = \left\{ \frac{E}{1-\nu^2}\begin{bmatrix} 1 & \nu \\ \nu & 1 \end{bmatrix} - \frac{1}{S}\begin{bmatrix} S_1^2 & S_1 S_2 \\ S_1 S_2 & S_2^2 \end{bmatrix} \right\}\begin{Bmatrix} d\varepsilon_1 \\ d\varepsilon_2 \end{Bmatrix} \tag{9}$$

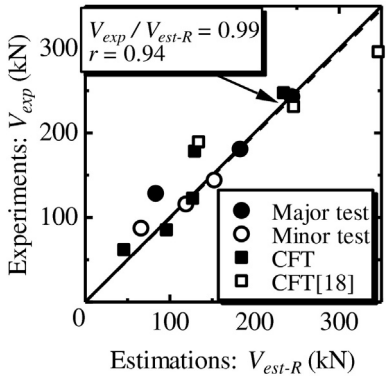

Fig. 9. Prediction and shear strength.

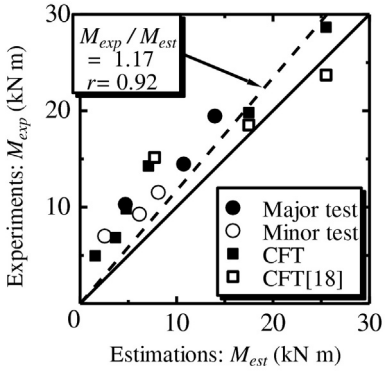

Fig. 10. Prediction and bending strength.

where S, S_1 and S_2 can be obtained as below,

$$S = s_1 S_1 + s_2 S_2, S_1 = \frac{E}{1-\nu^2}(s_1 + \nu s_2), S_2 = \frac{E}{1-\nu^2}(s_2 + \nu s_1) \tag{10a, b, c}$$

where s_1 and s_2 are stress deviators in the two principal directions.

Finally, the two elasto-plastic stresses can be obtained as below,

$$\sigma_1 = \sum d\sigma_1, \sigma_2 = \sum d\sigma_2 \tag{11a, b}$$

The two principal compressive stresses and strains are considered as positive.

The principal stress trajectories of major and minor axes test on CFEST subjected to bending-shear are shown in Fig. 12(a) and (b), in which the axes of the diagrams are normalized by the yielding point f_y. The broken line indicates the von Mises design criteria as expressed in Eq. (7). It can be seen from those figures that the two principal stresses flowed toward tensile and compressive region within the elastic range. The two principal stresses proceeded to tensile-tensile region after attaining yielding surface. This fact is explained in terms of the volumetric dilatation of in-filled concrete near the ultimate load.

Fig. 12(c) and (d) show the principal stress behavior of CFT tests. The axes of the diagrams are divided by f_y. The two principal stresses proceeded to tensile-tensile region owing to the volumetric dilatation of in-filled concrete, what coincides with the result of CFEST tests.

4. Conclusions

Bending-shear test on the concrete filled elliptical steel tubular deep beam subjected to bending and shear through asymmetric four-point loading test was conducted in order to be applied to the bridge pier. Additionally, shear strength of CFEST was compared with that of circular CFT having larger or smaller diameter of the CFEST. From the results, following conclusions are drawn.

1) Observed failure modes are cracking of the elliptical steel tube near the point of maximum bending tensile stress. With respect to the major test and circular CFT with $D = 160$ m specimens, shear failure of in-filled concrete between loading point and supports may be assumed.
2) Experimental shear strengths of the CFEST deep beam (V_{exp}) can be correctly predicted by the shear strength ($V_{est\text{-}R}$), which is the sum of concrete and steel tube shear strengths.
3) Experimental bending strength of the CFEST (M_{exp}) without confinement strength of in-filled concrete is, either in good agreement with, or larger than, the estimations.
4) The shear deformability of the two axes tests on the CFEST beams are strongly affected by diameter-to-thickness ratio of the elliptical steel tube. Additionally, the specimens with $t = 1.6$ mm approximately kept maximum values for the 5% displacement (δ/H).

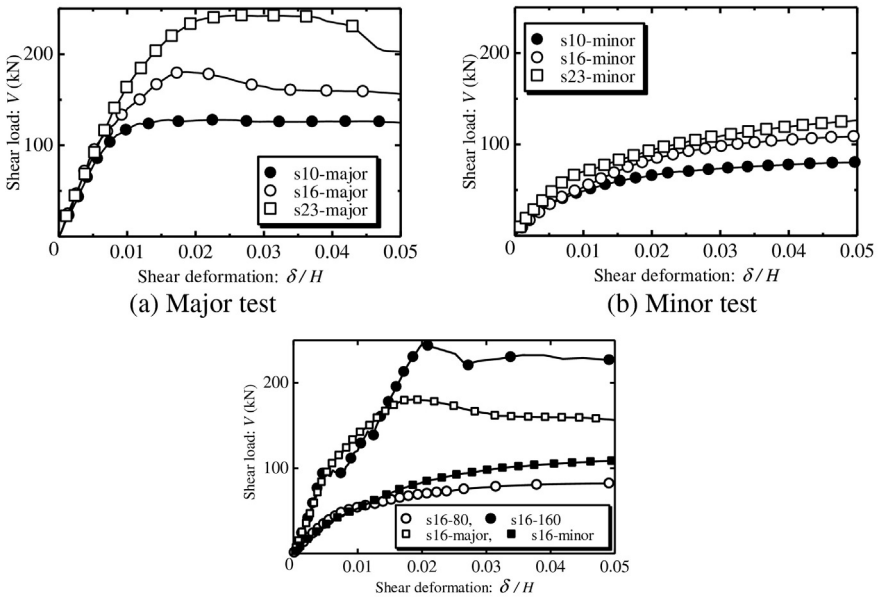

Fig. 11. Shear load versus displacement.

5) Shear deformability of the major and the minor test specimens decreased with the increase of diameter-to-thickness ratio.
6) The two principal stresses flowed toward tensile-compressive region within the elastic limit. The principal stresses proceeded to tensile-tensile region after yielding owing to volumetric dilatation of in-filled concrete.

Acknowledgment

We would like to thank Mr. Yoshitani, an Advanced Course Student on Kobe City College of Technology, for his sincere experimental assistance. We also thank Ms. Ichinose, manager of Infrastructure Maintenance Division of Japan Industrial Testing Corporation, for proof reading this manuscript.

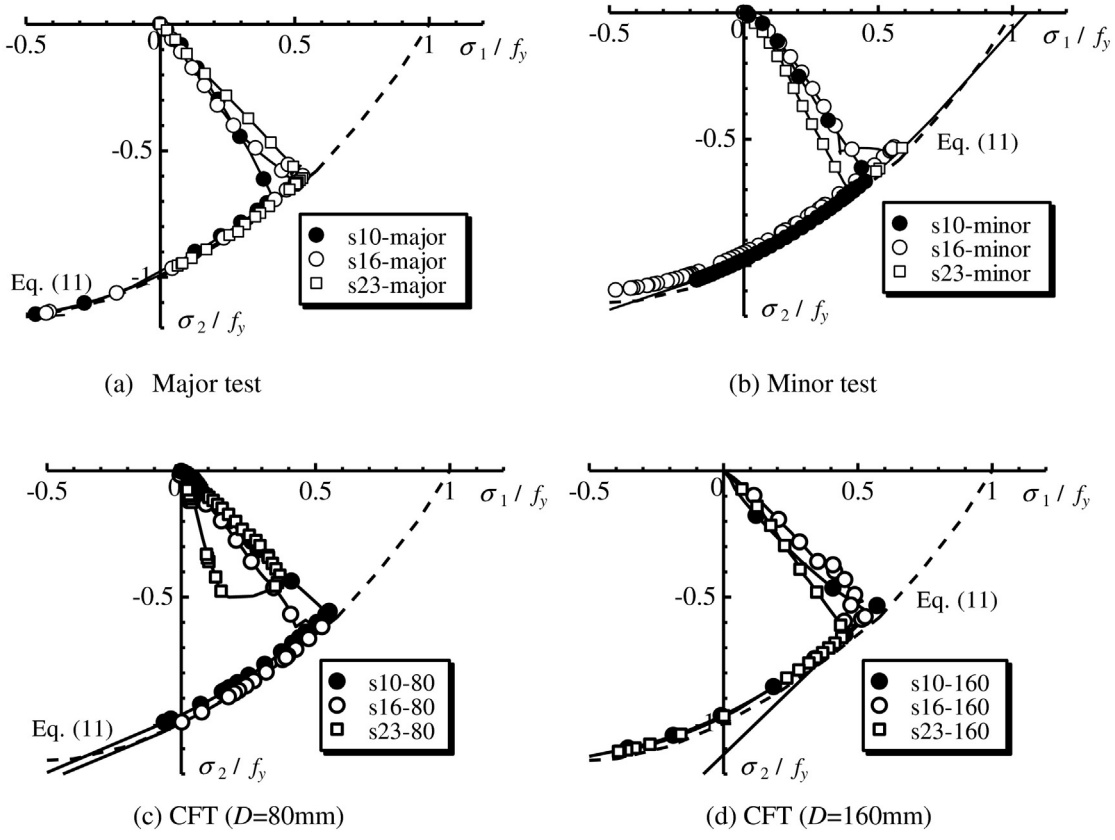

Fig. 12. Principal stress behavior.

References

[1] Architectural Institute of Japan. Standard for Structural Calculation of Steel Reinforced Concrete Structures. Maruzen; 2002(in Japanese).
[2] Architectural Institute of Japan. Recommendations for Design and Construction of Concrete Filled Steel Tubular Structures; 2008(in Japanese).
[3] Chan TM, Gardner L. Compressive resistance of hot-rolled elliptical hollow sections. Eng Struct 2008;30(2):522–32.
[4] Gardner L, Chan TM, Wadee MA. Shear response analysis of elliptical hollow sections. Struct Build 2008;161(SB6):301–9.
[5] Chan TM, Gardner L. Bending strength of hot-rolled elliptical hollow sections. J Constr Steel Res 2008;64:971–86.
[6] Ruiz-Teran AM, Gardner L. Elastic buckling of elliptical tubes. Thin-Walled Struct 2008;46:1304–18.
[7] Gardner L, Chan TM. Cross-section classification of elliptical hollow sections. Steel Compos Struct 2007;7(3):185–200.
[8] Yang H, Lam D, Gardner L. Testing and analysis of concrete-filled elliptical hollow section. Eng Struct 2008;30(12):3771–81.
[9] Zhao XL, Packer JA. Tests and design of concrete-filled elliptical hollow section stub columns. Thin-Walled Struct 2009;47(6–7):617–28.
[10] Chan TM, Huai YM, Wang W. Experimental investigation on lightweight concrete-filled cold-formed elliptical hollow section stub columns. J Constr Steel Res 2015; 115:434–44.
[11] Sheehan A, Dai XH, Chan TM, Lam D. Structural response of concrete-filled elliptical steel hollow sections under eccentric compression. Eng Struct 2012;45:314–23.
[12] McCann F, Gardner L, Qiu W. Experimental study of slender concrete-filled elliptical hollow section beam-columns. J Constr Steel Res 2015;113:185–94.
[13] Ren QX, Han LH, Lam D, Li W. Tests on elliptical concrete filled steel tubular (CFST) beams and columns. J Constr Steel Res 2014;99:149–60.
[14] Uenaka K. Experimental study on concrete filled elliptical/oval steel tubular stub columns under compression. Thin-Walled Struct 2014;78:131–7.
[15] Uenaka K, Tsunokake H. Concrete filled elliptical steel tubular members with large diameter-to-thickness ratio subjected to bending. Structures 2016;4:58–66.
[16] Uenaka K, Tsunokake H. Concrete filled elliptical steel tubular deep beam under bending and shear, Proceeding of the Japan Concrete Institute. 2015;37(2): 997–1002 (in Japanese).
[17] Niwa J. Design equations for ultimate shearing strength of deep RC beams based on FEM analysis. Proceedings of the 2nd colloquium on analytical problems of shearing mechanics of RC structure; 1983. p. 119–28 [in Japanese].
[18] Uenaka K. Concrete filled double skin circular tubular beams with large diameter-to-thickness ratio under shear. Thin-Walled Struct 2013;70:33–8.
[19] Japan Society of Civil Engineers. Introduction to Material Models of Material Characteristics-Terminology of Constitutive Laws; 1989(in Japanese).